A Mathematical Model of Imbibition for Two-Phase Flow in Porous Media using a Two-Dimensional Network Model

Kafi Shabbir[1], Oleg Izvekov[1], and Andrey Konyukhov[1]

[1]Moscow Institute of Physics and Technology

September 19, 2023

Abstract

Simulation of two-phase flow in porous media has many applications in oil recovery, hydrology, electricity production, etc. Classical continuum models consider permeability to be a function of only saturation. Classical continuum models are unable to explain non-equilibrium effects.

Advanced continuum models, such as the Kondaurov model considers permeability to be a function of a non-equilibrium parameter in addition to saturation. In order to better understand the non-equilibrium effects, it is necessary to develop non-continuum models at the scale of the pores, for example a network model.

This article is about the network model of two-phase flow in porous media which we developed, using which the saturation of the wetting phase with respect to time in the region of finer pores was calculated. A novel method for distributing phases at the nodes was used. According to the results obtained, the saturation rests to an equilibrium value.

The final objective of our research is to develop a network model in order to understand the physical meaning of the Kondaurov non-equilibrium parameter.

1 Introduction

Simulation of two-phase flow in porous media has applications in oil recovery, hydrology, electricity production where pressurised water is passed through heated pipes and is transformed into steam, etc. Hence it is important to understand and model two-phase flow in porous medium. [21]

1.1 Porous medium and capillary action

Figure 1 is an example of two-phase flow in porous media. The wetting fluid, in this case - water displaces the non wetting fluid - air, due to capillary action in the capillaries connecting the nodes, shown in figure 2.

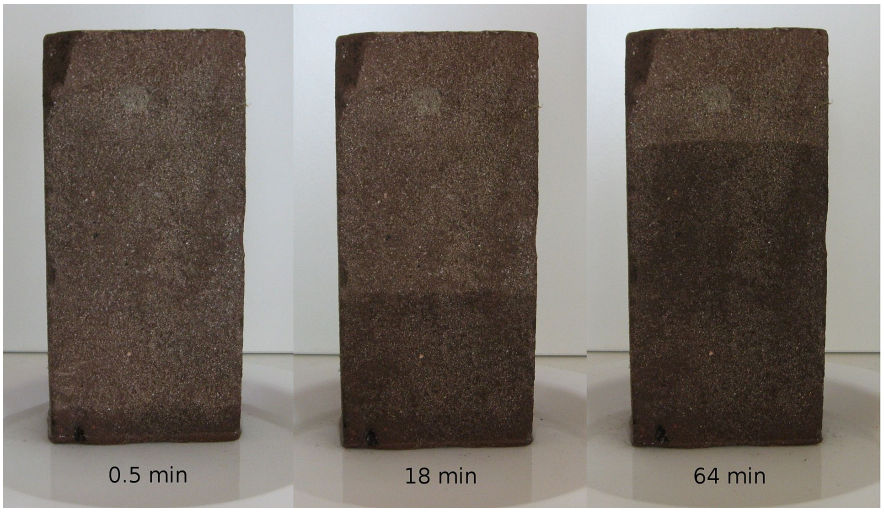

Figure 1: Water climbing against gravity through a porous medium due to capillary forces. [31]

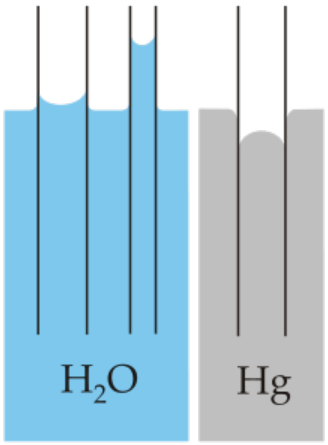

Figure 2: Showing capillary action of water (polar) compared to mercury (non-polar), with respect to a polar surface such as glass (Si–OH). [31]

1.2 Classical continuum models

Darcy's Law is a classical continuum model. It is given by:

$$q = -\frac{k}{\mu}\nabla p \tag{1}$$

Here, q is the flow rate, k is the permeability, μ is the coefficient of viscosity, ∇p is the pressure gradient.

The feature of these classical continuum models is that the permeability is only a function of the saturation of one of the phase.

$$k = k(S) \tag{2}$$

Here, k is the permeability as in equation 1, S is the saturation of one of the phase.

Saturation S is defined as the ratio between the volume occupied by a phase to the total volume of the void.

$$S = \frac{V_w}{V_{void}} \tag{3}$$

Here, V_w is volume occupied by the wetting phase, V_{void} is total volume of the void.

1.3 Advanced continuum models

The classical continuum models are valid as long as the characteristic time of the processes is much longer than the characteristic time of fluid redistribution in the capillary space.

When the saturation changes rapidly, or the porous medium has a structure such that the time of fluid redistribution is long. For example in fractured-porous medium with blocks and cracks, the assumption that $k = k(S)$ is not sufficient and additional parameters are required.

Various advanced continuum models that take these effects into account. Models of Hassanizadeh [10] [12] and Barenblatt [4] consider that, the permeability k is a function of the rate of saturation change $\frac{\partial S}{\partial t}$ in addition to the saturation S.

$$S = S(t) \tag{4}$$

$$k = k(S, \frac{\partial S}{\partial t}) \tag{5}$$

The Kondaurov model [19] considers a special non-equilibrium parameter ξ along with saturation S, which relaxes to an equilibrium value. [18]

$$k = k(S, \xi) \tag{6}$$

This parameter ξ is related to S by the differential equation:

$$\frac{\partial \xi}{\partial t} = \Omega(S, \xi) \tag{7}$$

The final objective of our network model is to understand the physical meaning of the non-equilibrium parameter ξ.

1.4 Non-continuum models

It is necessary to simulate the flow at the scale of pores, in order to better understand the non-equilibrium characteristics. Lattice Boltzmann Method, direct Navier-Stokes simulation or a network model are some of the methods of modelling at the scale of pores. Direct Navier-Stokes simulation provides but is very complicated. Network models are much simpler to model and perform computations than direct Navier–Stokes calculations.

One of the earliest models simulated the flow using a network of electrical resistors [8]. Some of the modern models simulated using hour glass shaped model of tubes [2], where the average flow rate is given by the Washburn equation for capillary flow [30], the disadvantage is that the flow rate must be approximated for cylindrical tube while in the model, the capillary pressure varies depending on its position in the tube.

The network model we developed uses cylindrical tubes, the flow rate is given by simple equations, also made use of a new method for distributing phases at the nodes. The applicability of our model in this article is shown by modelling imbibition.

2 Equations

2.1 Flow rate in a tube

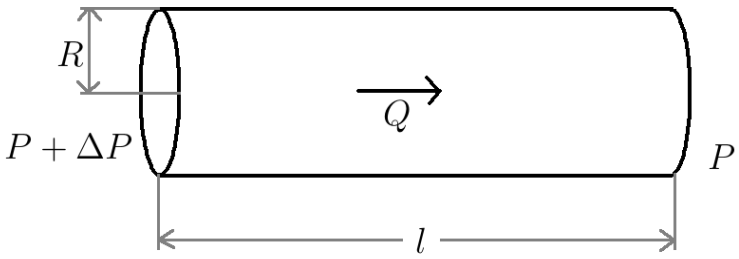

Figure 3: Tube with pressure difference across its ends causing fluid to flow.

The flow rate of a viscous fluid through a thin tube is given by the Hagen–Poiseuille equation:

$$Q = \frac{\pi}{8\mu}\frac{\Delta P}{l}R^4 \tag{8}$$

Here, Q is the volumetric flow rate in $[m^3/s]$, ΔP is the pressure difference between the ends of the tube, μ is the viscosity in $[kg/m.s]$, l is the length of the tube, R is the radius of the tube.

2.2 Flow rate in a tube with one meniscus

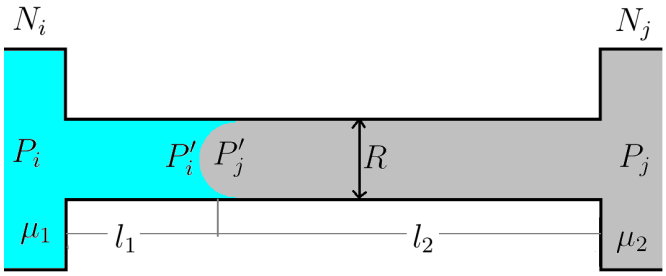

Figure 4: Orientation of the meniscus, the convex side contains wetting fluid while the concave side contains non-wetting fluid.

In figure 4, node N_i kept at a pressure of P_i, and is filled with a wetting fluid of viscosity μ_1. Node N_j kept at a pressure of P_j is filled with a non-wetting fluid of viscosity μ_2.

Since in figure 2 the wetting fluid rises against gravity, the pressure on the convex side of the meniscus is lower than on the concave side:

$$P_i' < P_j' \tag{9}$$

The pressure jump is given by:

$$P_j' - P_i' = \frac{2\sigma}{R} \tag{10}$$

Here, σ is the coefficient of surface tension in $[Pa.m]$ or $[kg/s]$.

In figure 4, when $P_i = P_j$, the fluids will flow from N_i to N_j due to the capillary pressure. Therefore, when $P_i > P_j$, the fluids will also move from N_i to N_j.

Separating figure 4 into two tubes of lengths l_1 and l_2, containing fluids of viscosity μ_1 and μ_2. The flow rates of the tubes, from equation 8 are given by:

$$Q_i = \frac{\pi}{8\mu_1}\frac{P_i - P_i^{'}}{l_1}R^4 \tag{11}$$

$$Q_j = \frac{\pi}{8\mu_2}\frac{P_j^{'} - P_j}{l_2}R^4 \tag{12}$$

The fluids are not compressible, then:

$$Q_i = Q_j = Q \tag{13}$$

Using equation 13, and multiplying equations 11 and 12 by $\mu_1 l_1$ and $\mu_2 l_2$ respectively:

$$Q\mu_1 l_1 = \frac{\pi}{8}(P_i - P_i^{'})R^4 \tag{14}$$

$$Q\mu_2 l_2 = \frac{\pi}{8}(P_j^{'} - P_j)R^4 \tag{15}$$

Adding equation 14 and 15:

$$Q(\mu_1 l_1 + \mu_2 l_2) = \frac{\pi}{8}R^4(P_i - P_j + P_j^{'} - P_i^{'}) \tag{16}$$

Let, the pressure difference between the nodes be defined as:

$$\Delta P_{ij} = P_i - P_j \tag{17}$$

Substituting 17 and 10 into equation 16, and after rearranging:

$$Q = \frac{\pi R^4}{8(\mu_1 l_1 + \mu_2 l_2)}\left(\Delta P_{ij} + \frac{2\sigma}{R}\right) \tag{18}$$

Defining M as the viscosity parameter:

$$M = \sum_k \mu_k \frac{l_k}{l} \tag{19}$$

Equation 18 becomes:

$$Q = \frac{\pi R^4}{8Ml}\left(\Delta P_{ij} + \frac{2\sigma}{R}\right) \tag{20}$$

2.3 Flow rate in a tube with multiple meniscus

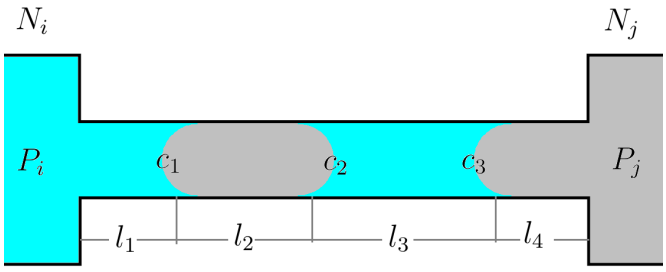

Figure 5: Capillary pressure contribution, $s = 1$

Let the capillary pressures be denoted by the following:

$$c_1 = -c_2 = c_3 = \frac{2\sigma}{R} \tag{21}$$

Then for figure 5, the flow rate is given by:

$$Q = \frac{\pi R^4}{8Ml} \left(\Delta P_{ij} + c_1 + c_2 + c_3 \right) \tag{22}$$

$$Q = \frac{\pi R^4}{8Ml} \left(\Delta P_{ij} + \sum_k c_k \right) \tag{23}$$

Flow rate for an arbitrary number of meniscus for a cylindrical tube, is given by:

$$Q = \frac{\pi R^4}{8Ml} \left(\Delta P_{ij} + \frac{2s\sigma}{R} \right) \tag{24}$$

Here s is defined as a function of orientation of the meniscus or the direction the convex side of the meniscus points d and the number of meniscus n_{mns}:

$$s(d, n_{mns}) = \begin{cases} -1, & n_{mns} = 1, \text{ convex side points away from } N_i \\ 0, & n_{mns} = 0,\ 2 \\ +1, & n_{mns} = 1, \text{ convex side points towards } N_i \end{cases} \tag{25}$$

In our model, the data structure does not accommodate more than 2 meniscus in a tube, therefore we limit the definition of s to a maximum of 2. s for various other configurations:

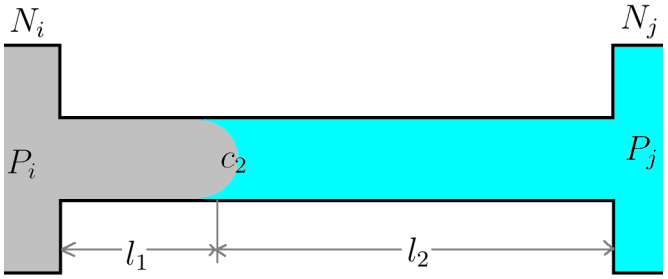

Figure 6: Capillary pressure contribution, $s = -1$

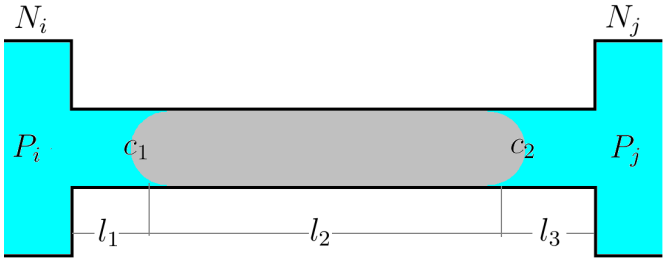

Figure 7: Capillary pressure contribution, $s = 0$

2.4 Set of linear equations for a node

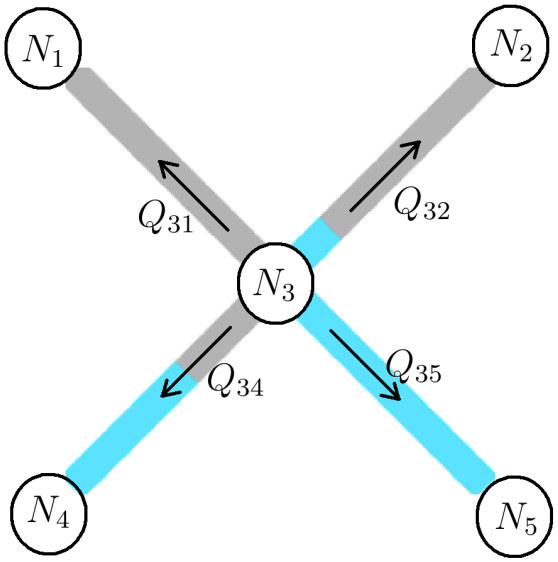

Figure 8: Capillary pressure contribution, $s = 0$

Let us apply our method on a simple system consisting of only 5 nodes. Note that all Q point outward. It is only to denote the direction. In order to preserve the law of conservation of volume, the Q's will have different signs.

Since there are 4 tubes, we can write 4 equations according to **??**

$$Q_{31} = \frac{\pi R_{31}^4}{8lM_{31}}(R_{31}\Delta P_{31} + 2s_{31}\sigma)$$

$$Q_{32} = \frac{\pi R_{32}^4}{8lM_{32}}(R_{32}\Delta P_{32} + 2s_{32}\sigma)$$

$$Q_{34} = \frac{\pi R_{34}^4}{8lM_{34}}(R_{34}\Delta P_{34} + 2s_{34}\sigma)$$

$$Q_{35} = \frac{\pi R_{35}^4}{8lM_{35}}(R_{35}\Delta P_{35} + 2s_{35}\sigma)$$

Due to the conservation of volume, we have:

$$\sum_k Q_{3k} = 0$$

Where $k = 1, 2, 4, 5$.

3 Features and characteristics of the model

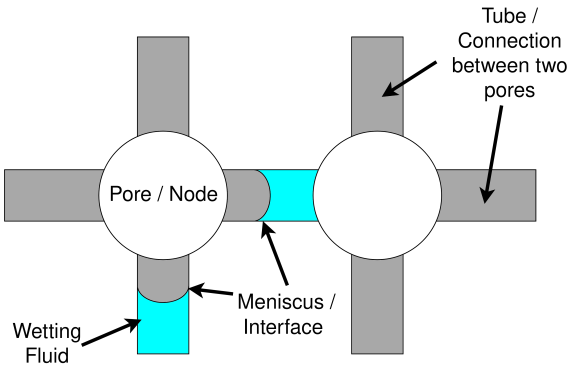

Figure showing two nodes from the network where the size of the node is much larger than the radius such that the capillary force tends to zero when the meniscus enters a node. In our model the volume of the pore is not taken into consideration. And all the capillaries which are denoted as tubes are cylindrical. All tubes are of equal length for simplicity.

3.1 Numbering tubes and other parameters in the network model

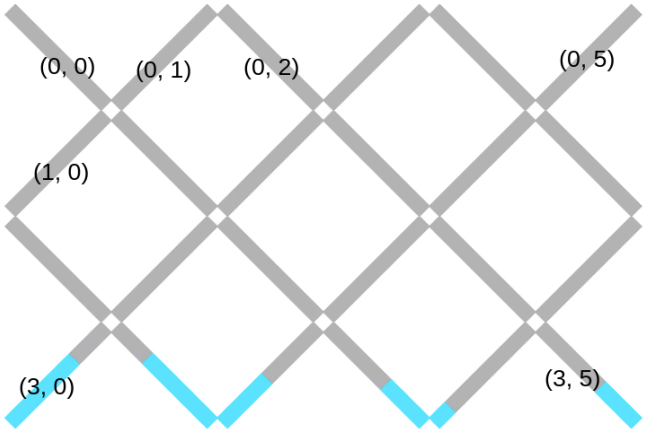

Figure 9: Numbering of tubes for a (rows, cols) = (4, 6) network model

If X is a parameter then X_{ij} is on the i th row and j th column, note that counting begins from zero. This type of counting is suitable for std::vector¡ data structure in C++.

3.2 Linear equations for simple displacement

In our model a node is connected to 4 tubes, or less if the node is located at the edges or a corner. The two-dimensional model can be extended to a three-

dimensional case similar to [25].

When generating the linear equations. For each row it is necessary to do the following for each direction:

$$[P_i] = [P_i] + R_{ij}K_{ij}$$
$$[P_j] = [P_j] - R_{ij}K_{ij}$$
$$[const] = [const] - 2s_{ij}\sigma K_{ij}$$

Here let $K_{ij} = R_{ij}^3/M_{ij}$.

For simplicity we rewrite the system of four equations as

In case of 5 nodes in our system, where the pressure of the bottom and top nodes are given and fixed, the matrix for Gaussian elimination will be:

$$\begin{pmatrix} 1 & 0 & 0 & 0 & 0 & P_{up} \\ 0 & 1 & 0 & 0 & 0 & P_{up} \\ -R_{31}K_{31} & -R_{32}K_{32} & (R_{3k}K_{3k}+...) & -R_{34}K_{34} & -R_{35}K_{35} & -2\sigma(s_{3k}K_{3k}+...) \\ 0 & 0 & 0 & 1 & 0 & P_{down} \\ 0 & 0 & 0 & 0 & 1 & P_{down} \end{pmatrix}$$

It can be proven that this matrix always has a solution. Once the solution is determined the flow rate can be calculated using equation **??**, and the velocity of flow in each tube is given by

$$\boxed{v_{ij} = \frac{R_{ij}}{8lM_{ij}}(R_{ij}\Delta P_{ij} + 2s_{ij}\sigma)} \tag{26}$$

3.3 Linear equations in case of infinitely many solutions

It is possible to calculate the pressures at each node, if the pressures are known on the edges. However when we want to model imhibition, the boundaries are closed and the total volume of a phase remains the same.

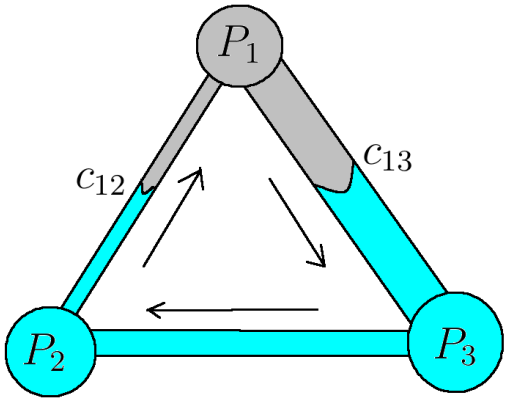

Figure 10: Case of of infinitely many solutions

Let the flow rates be given by:

$$q_{ij} = k_{ij}\Delta P + c_{ij} \tag{27}$$

For N_1:

$$q_{12} = k_{12}(P_1 - P_2) + c_{12}$$
$$q_{13} = k_{13}(P_1 - P_3) + c_{13}$$

Since:

$$q_{12} + q_{13} = 0$$
$$(k_{12} + k_{13})P_1 - k_{12}P_2 - k_{13}P_3 = -c_{12} - c_{13}$$

Then for each node we obtain the following matrix:

$$\begin{pmatrix} (k_{12}+k_{13}) & -k_{12} & -k_{13} & -c_{12}-c_{13} \\ -k_{21} & (k_{21}+k_{23}) & -k_{23} & -c_{21}-c_{23} \\ -k_{31} & -k_{32} & (k_{31}+k_{32}) & -c_{31}-c_{32} \end{pmatrix}$$

Note that:

$$k_{ij} = k_{ji}$$
$$c_{ij} = -c_{ji}$$

Hence the sum of each column of this matrix is zero.

By $R_3 = R_3 + R_1 + R_2$:

$$\begin{pmatrix} (k_{12}+k_{13}) & -k_{12} & -k_{13} & -c_{12}-c_{13} \\ -k_{21} & (k_{21}+k_{23}) & -k_{23} & -c_{21}-c_{23} \\ 0 & 0 & 0 & 0 \end{pmatrix}$$

This is solved by adding a constant a to one of the column of the matrix for each rows. In our model the centre was chosen to be the zero of pressure. Changing this point does not change the flow rates or the nature of flows.

$$\begin{pmatrix} (k_{12}+k_{13}) & -k_{12} & -k_{13}+a & -c_{12}-c_{13} \\ -k_{21} & (k_{21}+k_{23}) & -k_{23}+a & -c_{21}-c_{23} \\ -k_{31} & -k_{32} & (k_{31}+k_{32})+a & -c_{31}-c_{32} \end{pmatrix}$$

After $R_3 = R_3 + R_1 + R_2$:

$$\begin{pmatrix} (k_{12}+k_{13}) & -k_{12} & -k_{13}+a & -c_{12}-c_{13} \\ -k_{21} & (k_{21}+k_{23}) & -k_{23}+a & -c_{21}-c_{23} \\ 0 & 0 & 3a & 0 \end{pmatrix}$$

$$3aP_3 = 0$$

The solutions exists only if $P_3 = 0$.

3.4 Distribution and recombination

The novelty of our model is how we distribute phases in the nodes. When more than two phases flow into a node, the wetting fluid first enters the tube with the thinner radius. Our data structure was constrained to only allow the case for a maximum of two meniscus in a tube.

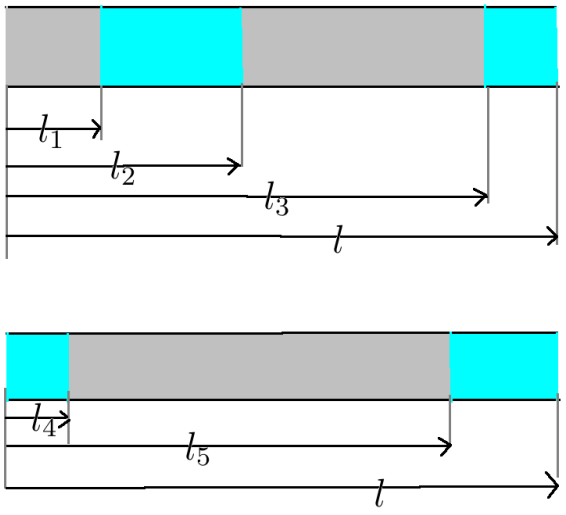

Figure 11: Case of more than two meniscus in a tube

Grey: $m_1 = l_1$ at $d_1 = \frac{l_1}{2}$,

$m_2 = l_3 - l_2$ at $d_2 = \frac{(l_3+l_2)}{2}$

$$m = m_1 + m_2$$
$$c_{grey} = \frac{m_1 d_1 + m_2 d_2}{m}$$

$$l_4 = c_{grey} - \frac{m}{2}$$
$$l_5 = l_4 + m$$

3.5 Algorithm for computation

1. **Input Files:** read input files, radius.txt and mns.txt, mns.txt contains the initial setup of the meniscus
2. **Random radius:** add very small random values to the radius, this is done in order to remove the case of two equal radius for simplicity, can be removed later
3. **Loop time:** do until a certain proportion of invading fluid is reached for example 0.90 or a fixed number of frames:
   (a) **Pressure:** determine the pressure at each node using the linear equations given in section 2.4.
   (b) **Velocity:** Calculate the velocity using equation 26
   (c) **time step:** determine the time step, it is the $\Delta t = minl/vi$.
   (d) **volume:** The volume displaced in each tube is determined by iterating through all the tubes, $V_{ij} = v_{ij} * t_{min}$.
   (e) **integration:**
      i. **Store insertion:** create a matrix to store how much of which fluid to insert in each of these tubes.
      ii. **Loop nodes:** Iterate through all the nodes, and for each of the nodes.
         A. divide the tubes into two categories, flow-in-tube - here the fluid from these tubes flow into the nodes, flow-out-tubes here we insert the fluid into the tube from the node
         B. Find out the total of fluid1, fluid2, which is the total of each fliud from all flow-in-tubes.
         C. Start filling the each of the flow-out-tubes where the flow will go into in ascending order of the radius of the tube. This will be done simply be adding the quantity of fluid1 and fluid2 to the matrix created above.

D. while filling fist use fluid1, once fluid1 is used up then start using fluid2, which means if in a tube we have to insert two fluids, then fluid1 will go in first.

iii. **Fluid addition:** For each of the tubes, add the volume of fluid determined to be added. After addition if there are more than 2 meniscus, then merge them retaining their center of masses.

(f) **Picture:** Save a picture of the current configuration.

4. Video: Make a video file from the pictures.

3.6 Possible Cases of Errors

3.6.1 Initial configuration for flow to start

The flow did not start when all the meniscus were located inside the nodes. Because in our model we assumed that there is not capillary pressure in the nodes. To overcome this, the meniscus were made to be situated inside the tubes.

3.6.2 Case of all meniscus located in the thick tubes

The solution of linear equation were such that, the capillary force balanced out the pressure gradient. The pressure was much higher outside in the thick tubes than in the thin tubes. Whether this was caused by error in the process of solving the linear equation or due to the initial setup, needs to be checked again. Error is, that it is impossible to determine whether the coefficient during the process of gauss elimination is zero or not. Because of the way how floating point numbers are handled by the CPU, 0 is often seen as a small number.

3.7 Simple tests for our model

3.7.1 Filtration

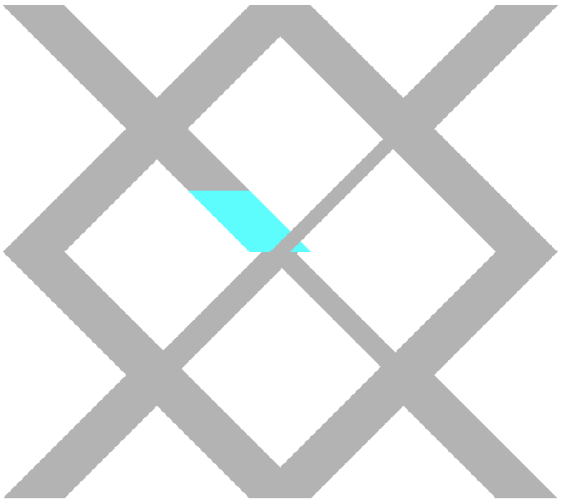

Figure 12: Initial position of wetting fluid

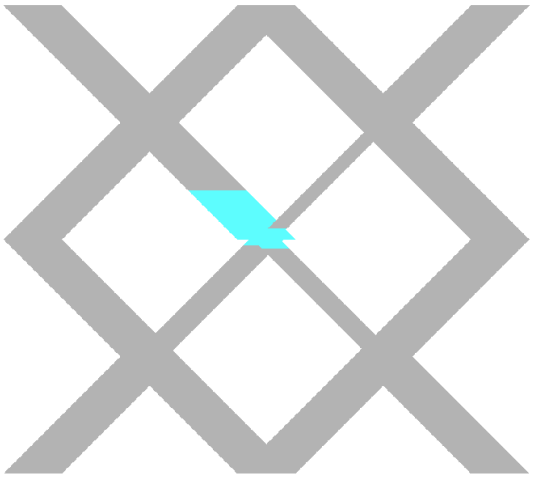

Figure 13: The wetting fluid chose to move to the tubes with thinner radius.

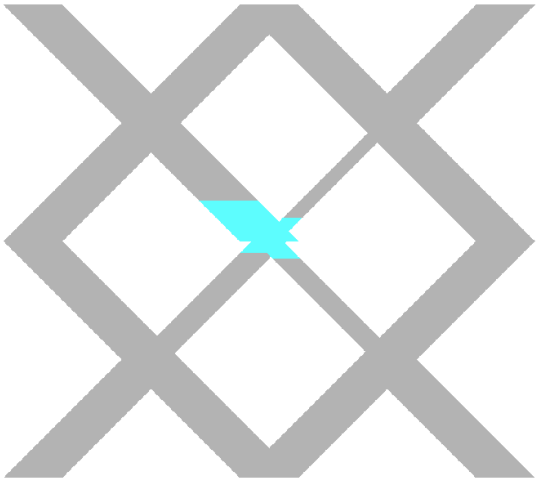

Figure 14: The flow accelerates as more fluid is in the thinner radius, here viscosity of the wetting fluid is higher.

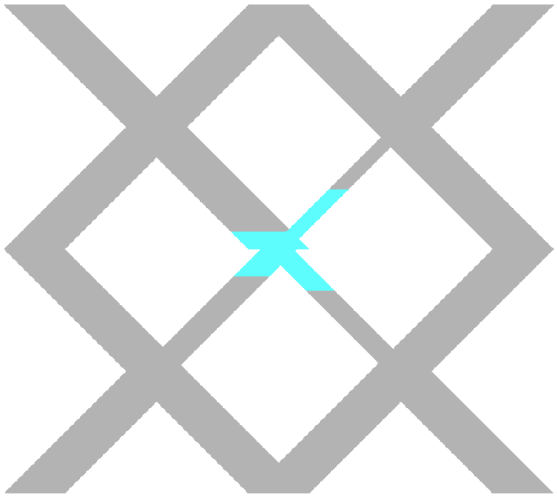

Figure 15

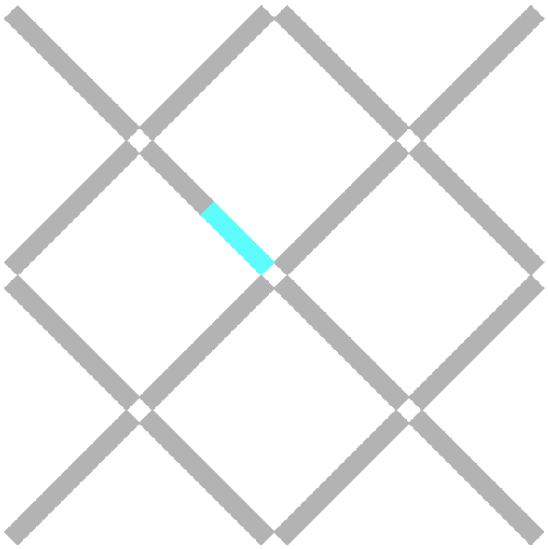

Figure 16: The same flow without plotting the radius thickness for clarity.

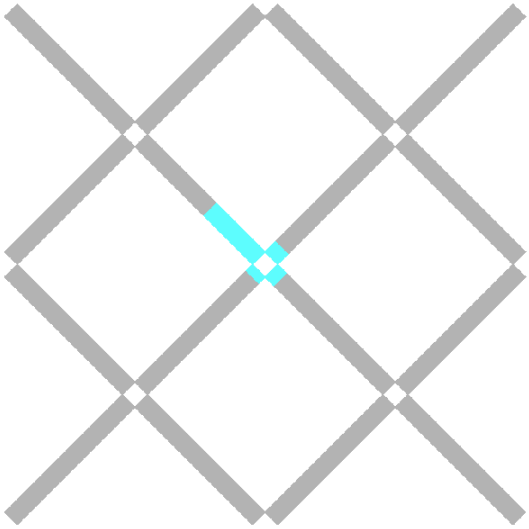

Figure 17

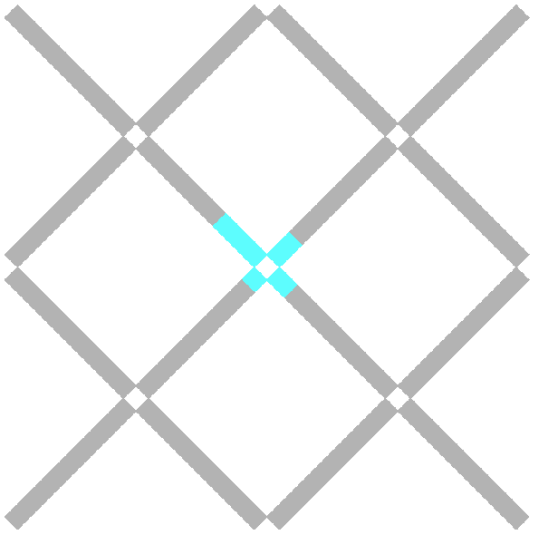

Figure 18

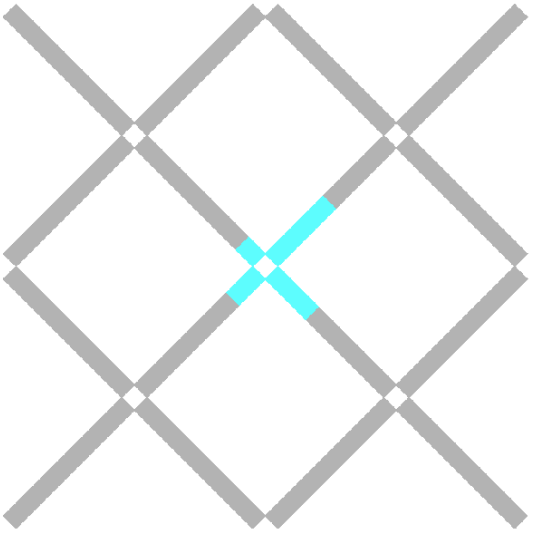

Figure 19

3.7.2 Displacement

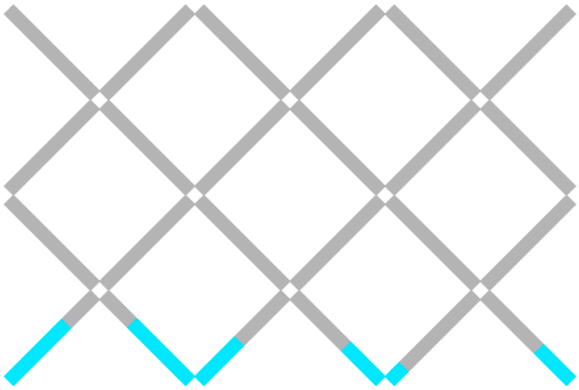

Figure 20: Our model is initially set up such that the wetting fluid is low in saturation and is confined to the bottom of our network. A higher pressure is fixed for all nodes at the bottom layer, while a low pressure is fixed for the top row.

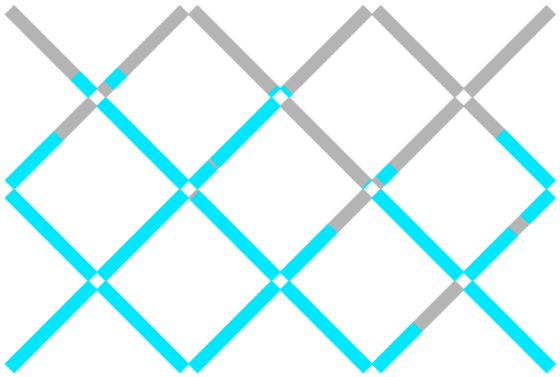

Figure 21: In all nodes, law of conservation of volume is applied, since mass is conserved and the phases are non-compressible. However for the bottom layer of nodes, the wetting fluid is injected as much required according to the sum of flow rates determined in the tubes connected to those nodes, while from the top layer of nodes a fluid is removed.

4 Simulation and results

4.1 Main Problem

- The aim of this simulation is observe the movement of wettable fluid (blue) from the region of thicker tube to the thinner tube.
- The saturation of each phase is measured in the region of thinner tubes.

- All boundaries are closed, the saturation of a phase for the whole system remains constant in time.
- The radius in the outer region is three times larger.

4.2 Result for Imbibition 10x10

4.2.1 Figures

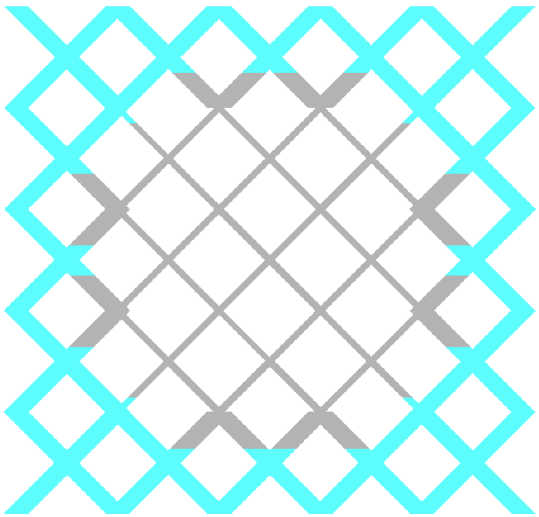

Figure 22: Initial setup, outer radius is 3 times larger than inner.

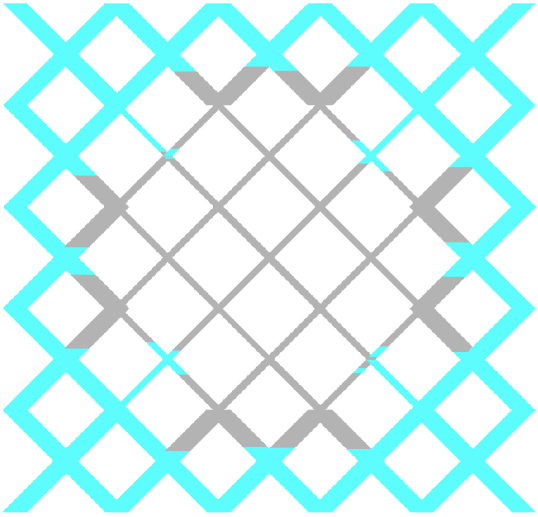

Figure 23: Showing invasion of wetting(blue) fluid into the region which contains thinner radius. The flow accelerates because, for a corner initially there are 3 meniscus, it multiplies into 3 when the meniscus reaches the node. The corner where the meniscus reaches the node late is pushed back because of the excessive pressures from the other corners.

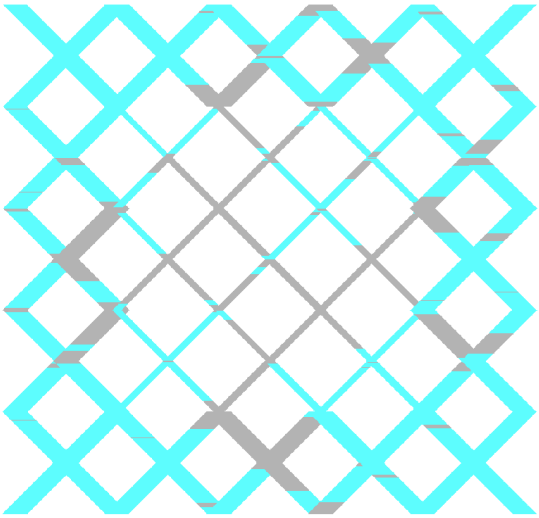

Figure 24: The invasion slows down and possibly oscillates, it is due to the meniscus in the inner region being ineffective to suck more blue fluid as most tubes have two meniscus. In our algorithm, tubes with two meniscus have a zero net pressure.

4.2.2 Plot

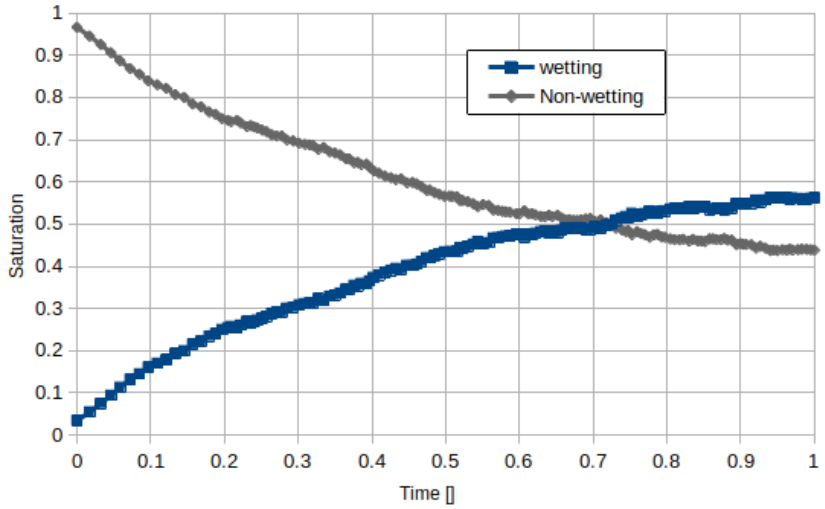

Figure 25: Plot of saturation of blue fluid in the region of thinner radius with respect to time, here the time is without dimensions.

For the simulations the length of each tube was taken to be unity and only the ratio of viscosity was used in equation **??**, since these values do not change the geometry of the flow and change only the scale of time. Dimensionless value of time was used.

4.2.3 Discussion

1. The blue fluid has approximately logarithmic dependence with time, the invasion rapidly rises and slows down, until it becomes almost constant. The calculation was stopped after 150 steps, because there was very small progress after it. Note that the time step for each step is different.
2. The blue fluid enters up to 0.56 of the saturation.
3. The saturation vs time appears similar to the ones in the reference [2], [8].

4.3 Result for Imbibition 26x26

4.3.1 Figures

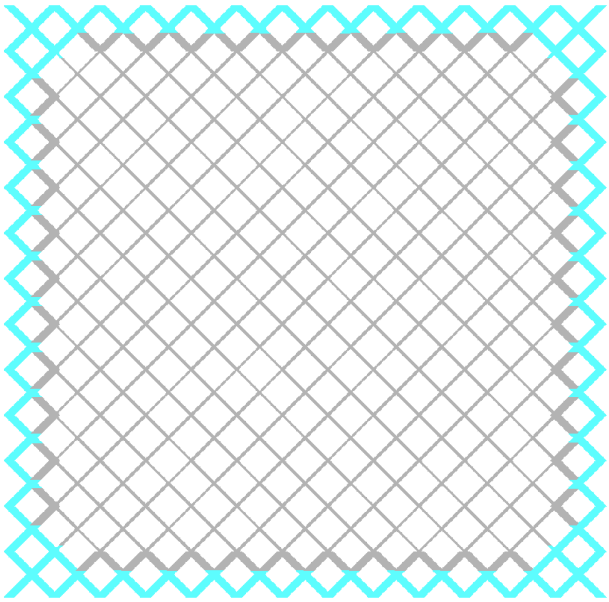

Figure 26: Initial setup

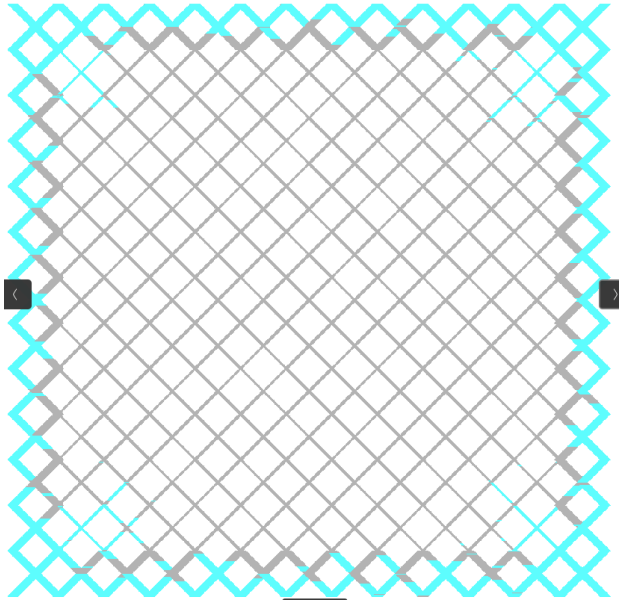

Figure 27: Acceleration

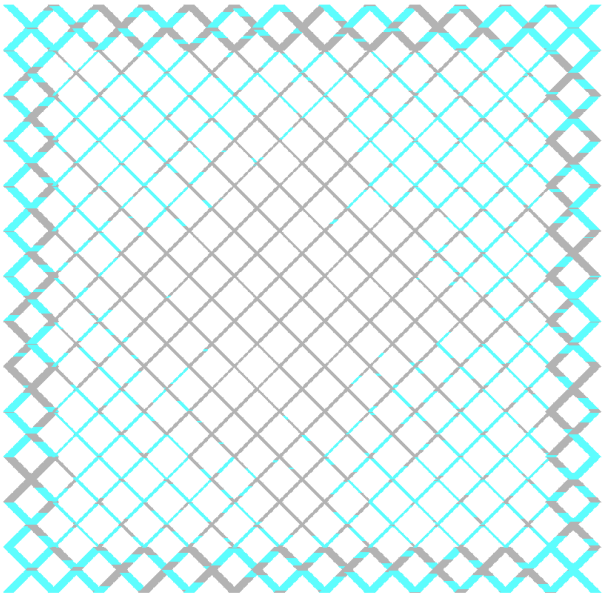

Figure 28: Slowing down

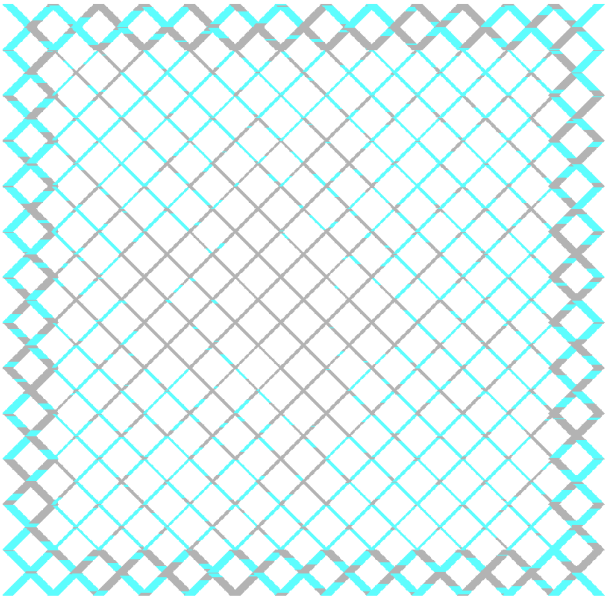

Figure 29: Final

4.3.2 Plot

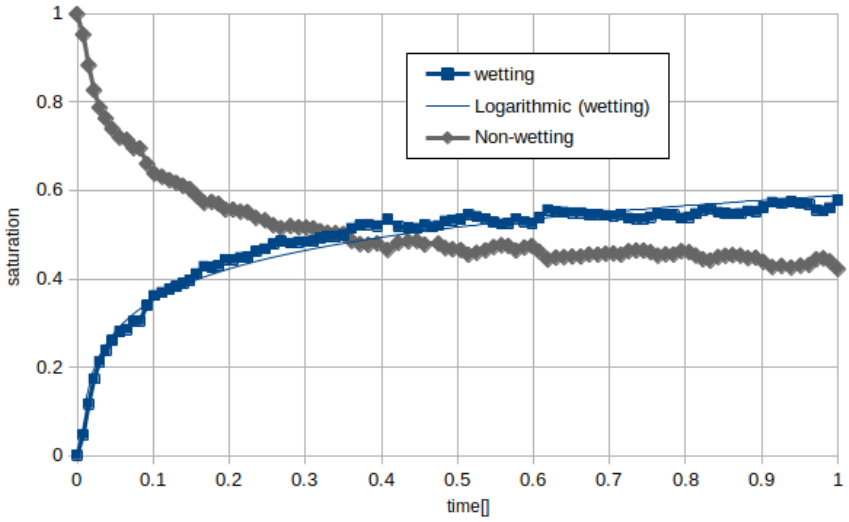

Figure 30: Plot of saturation of blue fluid in the region of thinner radius with respect to dimensionless time.

4.3.3 Discussion

1. Calculation was done for 20,000 steps.
2. Plot for every 200 frames.
3. Equal volumes of each phases.
4. The saturation for wetting fluid is 0.57 for the inner region, which is very close the previous simulation for 10x10.
5. It is clear that the relaxation parameter is present as the saturation converges to an equilibrium value.

5 Conclusions

1. The saturation of a phase in the inner region of the porous body tends to an equilibrium value.
2. The method of distributing fluid such the wetting fluid first goes to the tube with the thinner radius and calculating the flow rate using the modified Poiseuille equation is valid for explaining relaxation phenomena.
3. This algorithm can be extended to the case where there are more than 4 tubes connected to a node, since for two phase flow into a node case, we distribute in an ascending order of radii, in our model it is distributed to a maximum number to two tubes, but for hexagonal model it can be 4. We only need to update the function which produces the connections. The

same model can be used for a 3-dimensional case, where one surface has higher pressure than the opposite surface which has a lower pressure, it is to be used in order to more accurately represent the porous body.

4. Model of reasonable size can be simulated using Gaussian-elimination, which is more accurate than iterative methods.

5. The total volume for each phase for the whole system remains the same with the accuracy of 10^{-9}. Use of double is recommended instead of float.

6. Changing the ratio of viscosity affects the rate of displacement in the presence of pressure gradient, however in the case of inbibition significant differences were not observed.

7. The work will be continued as a part of Master's thesis. The ultimate goal is to verify the Kondaurov model, determine the physical meaning of the non equilibrium parameter, and the scope of its applicability.

References

[1] Cyrus K Aidun and Jonathan R Clausen. Lattice-boltzmann method for complex flows. *Annual review of fluid mechanics*, 42:439–472, 2010.

[2] Eyvind Aker, Knut JØrgen MÅlØy, Alex Hansen, and G George Batrouni. A two-dimensional network simulator for two-phase flow in porous media. *Transport in porous media*, 32:163–186, 1998.

[3] GI Barenblatt, TW Patzek, and DB Silin. The mathematical model of nonequilibrium effects in water-oil displacement. *SPE journal*, 8(04):409–416, 2003.

[4] Grigory I Barenblatt, Iu P Zheltov, and IN Kochina. Basic concepts in the theory of seepage of homogeneous liquids in fissured rocks [strata]. *Journal of applied mathematics and mechanics*, 24(5):1286–1303, 1960.

[5] Maria C Bravo and Mariela Araujo. Analysis of the unconventional behavior of oil relative permeability during depletion tests of gas-saturated heavy oils. *International journal of multiphase flow*, 34(5):447–460, 2008.

[6] Jing-Den Chen and David Wilkinson. Pore-scale viscous fingering in porous media. *Physical review letters*, 55(18):1892, 1985.

[7] Shiyi Chen and Gary D Doolen. Lattice boltzmann method for fluid flows. *Annual review of fluid mechanics*, 30(1):329–364, 1998.

[8] I Fatt. The network model of porous media. 3. dynamic properties of networks with tube radius distribution. *Transactions of the American institute of mining and metallurgical engineers*, 207(7):164–181, 1956.

[9] Yanbin Gong. *Dynamic Pore Network Modeling of Two-Phase Flow and Solute Transport in Disordered Porous Media and Rough-Walled Fractures*. University of Wyoming, 2021.

[10] S Majid Hassanizadeh. Continuum description of thermodynamic processes in porous media: Fundamentals and applications. *Modeling Coupled Phenomena in Saturated Porous Materials*, pages 179–223, 2004.

[11] S Majid Hassanizadeh, Michael A Celia, and Helge K Dahle. Dynamic effect in the capillary pressure–saturation relationship and its impacts on unsaturated flow. *Vadose Zone Journal*, 1(1):38–57, 2002.

[12] S Majid Hassanizadeh and William G Gray. High velocity flow in porous media. *Transport in porous media*, 2:521–531, 1987.

[13] S Majid Hassanizadeh and William G Gray. Mechanics and thermodynamics of multiphase flow in porous media including interphase boundaries. *Advances in water resources*, 13(4):169–186, 1990.

[14] S Majid Hassanizadeh and William G Gray. Thermodynamic basis of capillary pressure in porous media. *Water resources research*, 29(10):3389–3405, 1993.

[15] M King Hubbert. Darcy's law and the field equations of the flow of underground fluids. *Transactions of the AIME*, 207(01):222–239, 1956.

[16] V Joekar-Niasar, S Majid Hassanizadeh, and HK Dahle. Non-equilibrium effects in capillarity and interfacial area in two-phase flow: dynamic pore-network modelling. *Journal of fluid mechanics*, 655:38–71, 2010.

[17] PR King. The fractal nature of viscous fingering in porous media. *Journal of Physics A: Mathematical and General*, 20(8):L529, 1987.

[18] VI Kondaurov. The thermodynamically consistent equations of a thermoelastic saturated porous medium. *Journal of applied mathematics and mechanics*, 71(4):562–579, 2007.

[19] VI Kondaurov. A non-equilibrium model of a porous medium saturated with immiscible fluids. *Journal of Applied Mathematics and Mechanics*, 73(1):88–102, 2009.

[20] Andrey Konyukhov, Leonid Pankratov, and Anton Voloshin. The homogenized kondaurov type non-equilibrium model of two-phase flow in multiscale non-homogeneous media. *Physica Scripta*, 94(5):054002, 2019.

[21] N Labed, L Bennamoun, and JP Fohr. Experimental study of two-phase flow in porous media with measurement of relative permeability. *Fluid Dyn. Mater. Process*, 8(4):423–436, 2012.

[22] Stephen B Pope and Stephen B Pope. *Turbulent flows*. Cambridge university press, 2000.

[23] Harris Sajjad Rabbani. *Pore-scale investigation of wettability effects on two-phase flow in porous media*. The University of Manchester (United Kingdom), 2018.

[24] Amir Raoof and S Majid Hassanizadeh. A new method for generating pore-network models of porous media. *Transport in porous media*, 81:391–407, 2010.

[25] Santanu Sinha, Andrew T Bender, Matthew Danczyk, Kayla Keepseagle, Cody A Prather, Joshua M Bray, Linn W Thrane, Joseph D Seymour, Sarah L Codd, and Alex Hansen. Effective rheology of two-phase flow in three-dimensional porous media: experiment and simulation. *Transport in porous media*, 119:77–94, 2017.

[26] Cameron Tropea, Alexander L Yarin, John F Foss, et al. *Springer handbook of experimental fluid mechanics*, volume 1. Springer, 2007.

[27] Grétar Tryggvason, Bernard Bunner, Asghar Esmaeeli, Damir Juric, N Al-Rawahi, W Tauber, J Han, S Nas, and Y-J Jan. A front-tracking method for the computations of multiphase flow. *Journal of computational physics*, 169(2):708–759, 2001.

[28] Markus Uhlmann. An immersed boundary method with direct forcing for the simulation of particulate flows. *Journal of computational physics*, 209(2):448–476, 2005.

[29] Per H Valvatne and Martin J Blunt. Predictive pore-scale modeling of two-phase flow in mixed wet media. *Water resources research*, 40(7), 2004.

[30] Edward W Washburn. The dynamics of capillary flow. *Physical review*, 17(3):273, 1921.

[31] Wikipedia. Capillary action — Wikipedia, the free encyclopedia. `http://en.wikipedia.org/w/index.php?title=Capillary%20action&oldid=1155129318`, 2023. [Online; accessed 19-June-2023].

[32] Wahyu Perdana Yudistiawan, Sang Kyu Kwak, and Santosh Ansumali. Higher order galilean invariant lattice boltzmann model. In *The 6th International Conference for Mesoscopic Methods in Engineering and Science*, page 28, 2009.